Article

J. Biol. Regul. Homeost. Agents. 2024; 38(5): 3981–3990
https://doi.org/10.23812/j.biol.regul.homeost.agents.20243805.315

UBE2H Inhibits Pyroptosis in Microglia Cells following Ischemic Stroke by Mediating the Ubiquitination of *p53*/*CASP1*

Mingxing Guo[1], Qi Wang[2], Xin Sui[1], Li Li[3], Weiwei Jia[4], Yinan Tian[1], Qi Lu[1], Bo Wang[5], Yu Wang[1,*]

[1]Department of Neurology 2, Third Affiliated Hospital of Qiqihar Medical University, 161000 Qiqihar, Heilongjiang, China
[2]Department of Immunology, College of Medical Technology, Qiqihar Medical University, 161000 Qiqihar, Heilongjiang, China
[3]Basic Medical Department of Qiqihar Medical University, 161000 Qiqihar, Heilongjiang, China
[4]Research Laboratory of Basic Medical School, Qiqihar Medical University, 161000 Qiqihar, Heilongjiang, China
[5]Department of Neurology 3, Third Affiliated Hospital of Qiqihar Medical University, 161000 Qiqihar, Heilongjiang, China
*Correspondence: aminda001@qmu.edu.cn (Yu Wang)
Published: 1 May 2024

Background: Ischemic stroke is the leading cause of permanent disability, affecting approximately 14 million people annually. Therefore, this study aimed to elucidate the role and underlying mechanism of *p53*/cysteinyl aspartate specific proteinase 1 (*CASP1*) in ischemic stroke.

Methods: The raw data regarding ischemic stroke were acquired from the GSE97537 data set of Gene Expression Omnibus (GEO). Moreover, a mouse model of cerebral ischemia was established. Neurons and microglia cells were used for *in vitro* experiments. Quantitative polymerase chain reaction (qPCR) and western blot analysis were used to assess the expression levels of target genes.

Results: We observed that ubiquitinconjugating enzyme E2H (*UBE2H*) expression was downregulated following ischemic stroke. The expression of *UBE2H* was found to promote pyroptosis of microglia cells. Furthermore, a negative correlation was observed between *CASP1* and *UBE2H*. The inhibition of *CASP1* significantly reduced pyroptosis, while the inhibition of *UBE2H* increased *CASP1* activity in microglia. Additionally, we observed a close association between elevated *CASP1* expression and poorer survival in ischemic stroke.

Conclusions: In summary, this study indicates that *UBE2H* inhibits microglial apoptosis following ischemic stroke by mediating the ubiquitination of *p53*/*CASP1*.

Keywords: *UBE2H*; pyroptosis of microglia cells; ischemic stroke; *p53*/*CASP1*

Introduction

Ischemic stroke accounts for approximately 87% of all stroke types and is characterized by the obstruction of fluid flow due to blood clots or embolism blocking blood vessels that supply specific areas [1]. Ischemic stroke is the leading cause of permanent disability, affecting approximately 14 million people annually [2]. There is increasing evidence indicating that inflammation after ischemia serves as a secondary progression of brain injury, and the severity of stroke outcomes in patients with comorbid conditions depends on the degree of this inflammatory response [3–5]. Cell death and brain tissue damage induce the activation of additional Microglia and the recruitment of infiltrating leukocytes, releasing more proinflammatory factors, thereby increasing the inflammatory response [6]. This inflammation, in turn, aggravates brain edema and hemorrhage, increases damage to blood-brain barrier, and promotes neural death [7]. On the contrary, neuroinflammation can promote the repair of brain damage by promoting neurogenesis and angiogenesis [8]. Therefore, it is necessary to explore post-stroke inflammation to improve the treatment and prognosis of ischemic stroke.

Pyroptosis is a form of programmed cell death-inducing cell lysis and inflammation, usually triggered by inflammasomes and executed by gasdermin proteins. The main characteristics of pyroptosis include cell swelling, membrane perforation, and the release of cellular contents. However, during normal physiology conditions, pyroptosis is critical in host defense against pathogen infection. Furthermore, cysteinyl aspartate specific proteinase 1 (*CASP1*), a member of the caspase family, was initially identified in the human monocyte cell line THP1 and has been recognized as a key enzyme of the pyroptosis pathway [9,10]. *CASP1* has been found to participate in proteolysis, protein auto-processing, pyroptosis, and several vital sig-

Journal of
BIOLOGICAL REGULATORS
and Homeostatic Agents

naling pathways [11–13]. Additionally, *p53* is known as the guardian of the genome. *p53* becomes activated in response to various stress signals, including DNA damage or oncogene activation, and orchestrates many downstream responses, such as DNA repair, cell cycle arrest, senescence, metabolism, and cell death. Furthermore, *p53* mainly acts as a transcription factor, controlling the expression of numerous target genes [14].

Proteins are categorized through ubiquitination, a cascade reaction of E1, E2, and E3 enzymes specifically modifying target proteins [15]. Ubiquitination is associated with various cardiovascular and cerebrovascular diseases in humans [16]. It has been reported that ubiquitinconjugating enzyme E2H (*UBE2H*) has high transcriptional levels in Alzheimer's disease (AD) patients [17]. *UBE2H* has become a drug target for many new drugs, presenting binding sites for nuclear factor kappa-B (NF-κB) and tumor necrosis factor-α (TNF-α). Additionally, it has been indicated to stimulate the expression of *UBE2H* in mouse muscles [18]. Furthermore, recent genetic studies have demonstrated a potential correlation between *UBE2H* and neurodegenerative diseases. Bioinformatics analysis has shown downregulation of *UBE2H* expression after ischemic stroke [19]. However, the function of this gene remains poorly understood at the cellular and biological levels, with limited studies focusing on *UBE2H* in ischemic stroke.

This study explored the expression patterns of *UBE2H* in ischemic stroke utilizing the combination of bioinformatics analysis and various experimental methods. Furthermore, it elucidated the regulatory mechanism of *UBE2H* in microglial pyroptosis. Therefore, investigating *UBE2H* helps explore the occurrence and development of ischemic stroke and identify potential diagnostic and therapeutic targets for this disease.

Methods

Data Collection and Identification of DEGs

The GSE97537 data set regarding ischemic stroke was acquired from Gene Expression Omnibus (GEO, available at: https://www.ncbi.nlm.nih.gov/geo/) using the GEOquery R package (version 3.1.3, https://www.bioconductor.org/packages/release/bioc/vignettes/GEOquery/). This data set comprises 12 samples, including 5 control samples and 7 Middle Cerebral Artery Occlusion (MCAO) samples, documented under the data platform GPL1355. However, the expression profile was normalized and standardized using the limma R package (version 4.0.2, The R Foundation for Statistical Computing, Vienna, Austria). Furthermore, differentially expressed genes (DEGs) were identified using a limma package. Subsequently, correlation analysis was performed using R software (version 4.1.0, R Foundation for Statistical Computing, Vienna, Austria) with ggplot2 and ggpubr, resulting in the acquisition of the Pearson correlation coefficient (r). Furthermore, to evaluate the pyroptosis level in ischemic stroke, pyroptosis-related genes were extracted from a prior study, and the pyroptosis score was determined using single-sample gene set enrichment analysis (ssGSEA) in the R 'performed gene set variation analysis (GSVA)' package.

Animal Experiment

A total of 18 C57BL/6J male mice and 18 CX3CR-CRE mice, aged 7 weeks and weighing 23 g–25 g, were obtained from Jackson Laboratory, Bar Harbor (Lansing, MI, USA). The mice were maintained in a controlled environment with a 12-hour light-dark cycle, keeping the temperature at approximately 22 °C and the relative humidity at 40%, ensuring adequate physical resources. They were randomly divided into the MCAO group and the blank group. Despite the random grouping of mice, there was no crossing between these two groups. All experiments involving mice were approved by the Ethical Committee of the Third Affiliated Hospital of Qiqihar Medical University, China (No. AECC-2022-006).

Establishment of a Short-Term Cerebral Ischemia Mouse Model

A short-term cerebral ischemia mouse model was established following a previously described method. The male mice received 100 mg/kg of 4% pentobarbital sodium (CAS#: 57-33-0, China National Pharmaceutical Group Chemical Reagent Co., Ltd., Shanghai, China) through the vein and exposed the arteries on the left side of the neck, including External Cartied Artery (ECA), Internal Cartied Artery (ICA), and Common Cartied Artery (CCA). The remote ends of the CCA and ECA were ligated with two surrounding nylons. Subsequently, an incision was created on the catheter at the ECA ligation site, and a 2 cm long nylon wire from the ECA was inserted into the lumen of the ICA, marking its position at 1 cm depth. Furthermore, cerebral blood flow was monitored using a laser Doppler flow meter. Ischemia-Reperfusion (I/R) is the reduction of at least 75% from the baseline blood flow at the onset of ischemia and 50% of the baseline blood flow measurement. However, the mice failing to reach these criteria were excluded from the study. After 1 hour of ischemia, the pliers were removed for re-injection. Furthermore, for the control group, mice underwent the same surgical procedures but without occlusion of blood vessels. At 0 hour, 12 hours, 24 hours, and 30 hours, 5 mice were euthanized at each time point. For this purpose, mice were suffocated in a closed container using CO_2 and other gases. After this, the mouse's brain tissue was excised promptly and stored at –20 °C for subsequent analysis.

Establishment of Oxygen-Glucose Deprivation/Reoxygenation (OGD/R) Model

The mouse microglial BV-2 cell line (product number: ZQ0397) and human neuroblastoma cell line SH-SY5Y

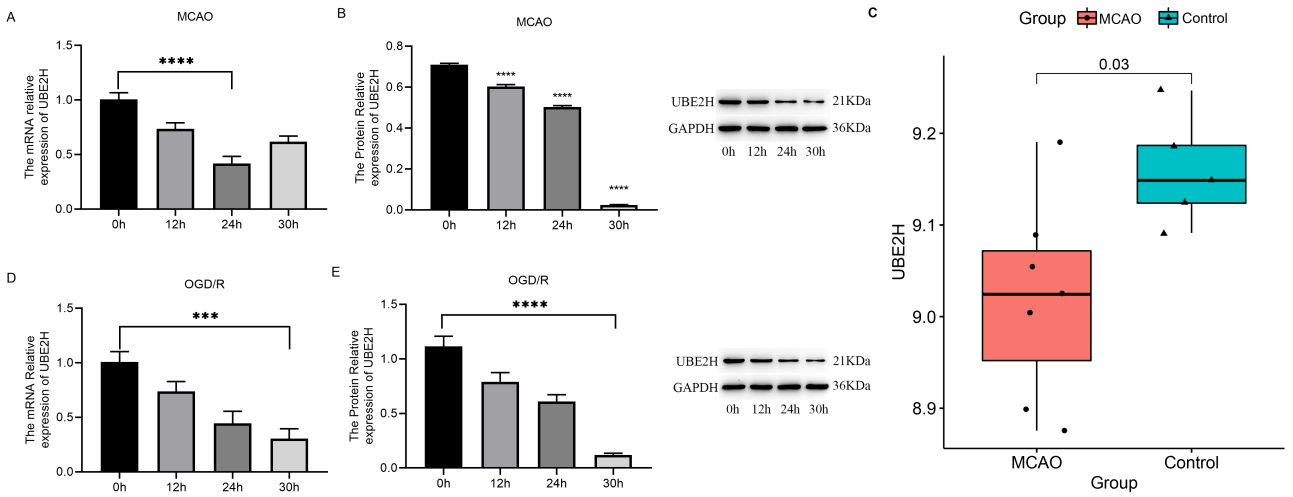

Fig. 1. Expression of *UBE2H* mRNA and protein in brain tissues and cells at different treatment times. (A) The expression levels of *UBE2H* mRNA in brain tissue using quantitative real-time polymerase chain reaction (qRT-PCR). (B) The expression levels of UBE2H protein in mouse brain tissue were treated at different Ischemia-Reperfusion (I/R) times. (C) The GSE97537 data analysis. (D) *UBE2H* expression levels in cells treated with different oxygen-glucose deprivation/reoxygenation (OGD/R) times. (E) UBE2H protein expression in cells treated with different OGD/R times. n = 6, ***$p < 0.001$, ****$p < 0.0001$.

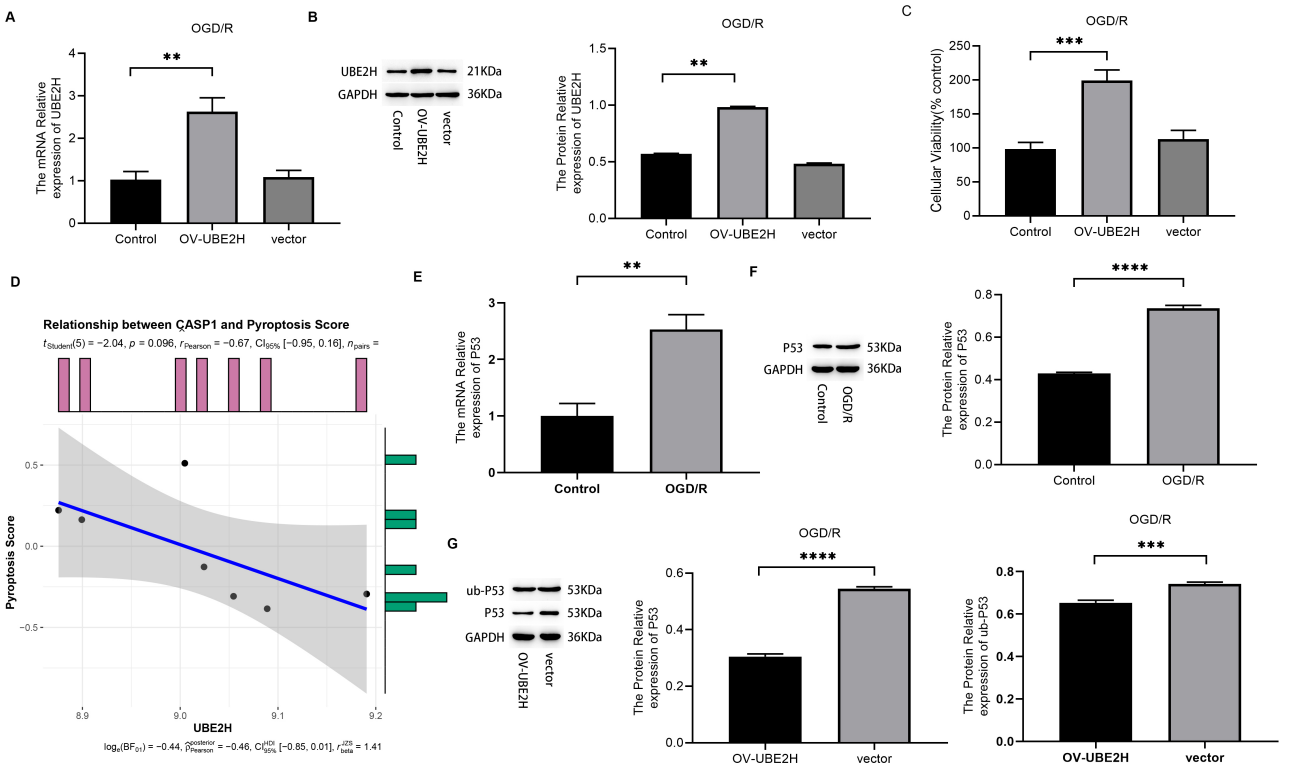

Fig. 2. *UBE2H* overexpression induced pyroptosis in microglia cells under OGD/R. (A,B) qRT-PCR and western blot (WB) analysis of the *UBE2H* expression in cells of each group following *UBE2H* overexpression. (C) Cell viability levels in each group of cells. (D) Kyoto Encyclopedia of Genes and Genomes (KEGG) pathway analysis. (E,F) qRT-PCR and protein analysis of *p53*. (G) *p53* expression in cells after *UBE2H* overexpression. n = 6, **$p < 0.01$, ***$p < 0.001$, ****$p < 0.0001$.

(product number: ZQ0050) were purchased from Shanghai Zhong Qiao Xin Zhou Co., Ltd., Shanghai, China. BV-2 cells were cultured in MEM medium (item number: ZQ-300, Shanghai Zhong Qiao Xin Zhou Co., Ltd., Shanghai, China) supplemented with 10% fetal bovine serum (FBS, 1693361, Gibco, Grand Island, NY, USA), 100 U/mL

Journal of
BIOLOGICAL REGULATORS
and Homeostatic Agents

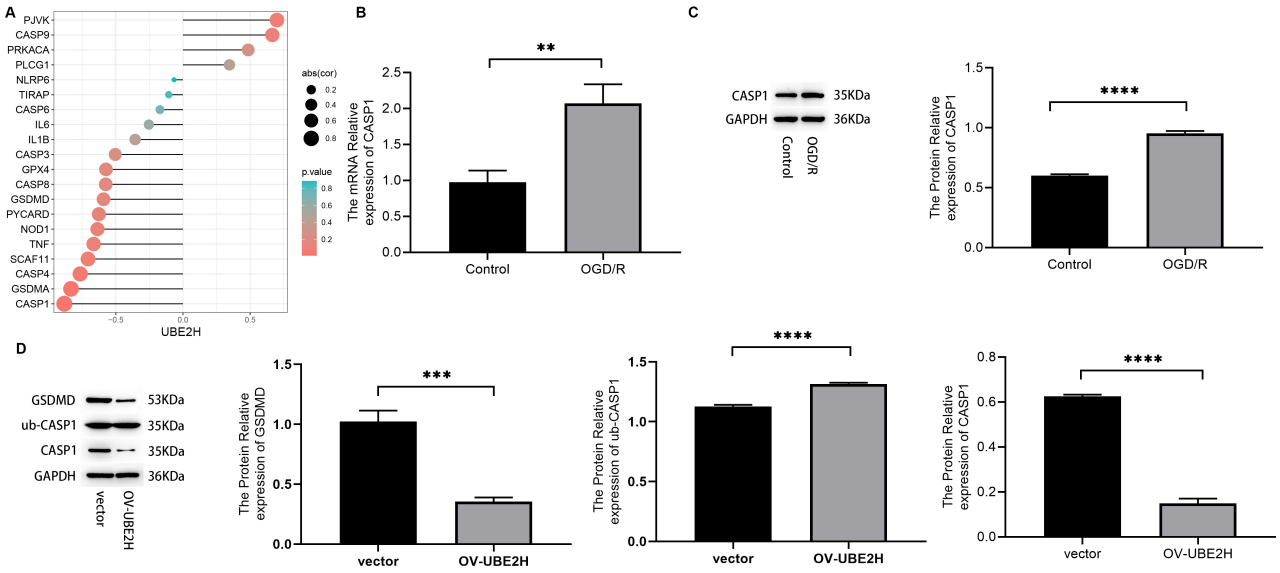

Fig. 3. *UBE2H* regulates pyroptosis in microglial through *CASP1*. (A) Screening of *CASP1* as a target gene. (B) qRT-PCR analysis of the *CASP1* levels. (C) Western blot analysis of the *CASP1* levels. (D) Western blot analysis of *CASP1* and Gasdermin D (*GSDMD*) expression after *UBE2H* overexpression. n = 6, $^{**}p < 0.01$, $^{***}p < 0.001$, $^{****}p < 0.0001$.

penicillin, and 100 U/mL streptomycin. However, SH-SY5Y cells were cultured in MEM/F12 complete medium (cat. ZQ-1205, Shanghai Zhong Qiao Xin Zhou Co., Ltd., Shanghai, China). The cells were incubated in a humidified atmosphere of 5% CO_2 at 37 °C for 2 hours. Additionally, the cells were cultured in Dulbecco modified eagle medium (DMEM) containing 10% FBS (Sigma Aldrich, St. Louis, MO, USA) at 37 °C and 5% CO_2 and subsequently underwent transfection using Lipofectamine 3000 reagent (Thermo Fisher Scientific, Waltham, MA, USA). Furthermore, the cells were cultured in glucose-free DMEM followed by incubation at 37 °C in the presence of 5% carbon dioxide and 95% nitrogen. The cells were collected following 0 hour, 6 hours, 12 hours, and 24 hours of combined oxygen therapy for subsequent analysis. The cells were authenticated using STR profiling and found no cross contamination utilizing mycoplasma testing.

Determination of Cerebral Water Content, Cerebral Index, and Cerebral Infarction in Mice

The wet and dry weight method was used during these experiments. After 24 h of ischemia/reperfusion, male mice underwent excessive anesthesia by intravenously administering 200 mg/kg of 4% pentobarbital sodium (CAS#: 57-33-0, China Pharmaceutical Group Chemical Reagent Co., Ltd., Shanghai, China). Subsequently, the brains were gently excised upon decapitation, with the olfactory bulb, cerebellum, and low brainstem being removed. The left and right cerebral hemispheres were separated, and their wet weights were recorded. After this, the brain tissues were heated in an electric oven at 110 °C for 24 hours, and their dry weights were then assessed. The cerebral water content (%) was determined using the following formula: (wet weight – dry weight)/wet weight × 100%. Moreover, the cerebral index was determined as follows: cerebral wet mass/body mass.

The brain tissues from mice were excised and frozen at –20 °C for 30 minutes. The tissues were sliced into 2 mm thick sections and subsequently stained with 2.0% 3,5-triphenyl-2H-tetrazolium chloride (TTC) solution for 30 minutes. The stained tissue sections were washed with phosphate-buffered saline (PBS) buffer and then overnight incubated in 4% paraformaldehyde at 4 °C for fixation. Normal brain tissue sections, after TTC staining, showed a pink hue, while infarcted areas appeared off-white. The infarct volume of each brain slice was assessed using Image J software (version 1.4.3.67, National Institutes of Health, Bethesda, MD, USA). The infarct volume was calculated as follows: infarct area × thickness/2.

Cell and Model Processing

Under OGD/R conditions, microglia underwent various manipulations, including CASP1 activation (OV-CASP1), CASP1 knockout (si-CASP1), *UBE2H* activation (OV-*UBE2H*), *UBE2H* knockout (si-*UBE2H*), and co-transfection of CASP1 and *UBE2H* using Lipofectamine 2000 reagent (product number: 11668030, Thermo, Waltham, MA, USA). Simultaneously, experimental stroke model group (MCAO), blank group (Control), experimental ischemic model p53 inhibitor group (MCAO+p53 inhibitor, 10 uM/days), and experimental cerebral infarction model+CASP1 inhibitor group (MCAO+CASP1 inhibitor, 10 uM/days) were established using MCAO surgery. The plasmid and vector were obtained from Thermo Scientific

Table 1. A list of primers used in qPCR.

Primer name	Primer sequence
UBE2H	F: 5′-ATGTACCTCCACCGACCAGA-3′
UBE2H	R: 5′-ACTCCATATCCTGGGCCTCA-3′
CASP1	F: 5′-GCCTGCCGTGGTGATAATGT-3′
CASP1	R: 3′-TCACTCTTTCAGTGGTGGGC-5′
p53	F: 5′-AACCGCCGACCTATCCTTACC-3′
p53	R: 5′-GCACAAACACGAACCTCAAAGC-3′
GAPDH	F: 5′-GTGGCAAAGTGGAGATTGTTG-3′
GAPDH	R: 5′-CGTTGAATTTGCCGTGAGTG-3′

qPCR, quantitative polymerase chain reaction; *CASP1*, cysteinyl aspartate specific proteinase 1; *GAPDH*, glyceraldehyde-3-phosphate dehydrogenase; *UBE2H*, ubiquitinconjugating enzyme E2H.

(product numbers: V79020, AM16708, Waltham, MA, USA), while p53 inhibitors were purchased from MCE Company (HY-70027, New Jersey, CA, USA).

Cell Counting Kit-8 (CCK-8) Assay

The cells were seeded into 96 well plates at a density of 5×10^3 cells/well, followed by overnight incubation. The next day, when cells have completely adhered to the wall, fluid exchange and dosing treatment were performed, adjusting the corresponding drug concentration. After preparation, the supernatant was removed from the 96-well plate, and 100 μL of the corresponding drug concentration medium was added to each well. Following 24 hours of incubation, 10 μL of CCK-8 reagent (C0037, Beyotime Biological Co., Ltd., Shanghai, China) was added to each well, and the absorbance (OD) at 450 nm was assessed employing a microplate reader (E0226, Beyotime Biological Co., Ltd., Shanghai, China).

Quantitative Polymerase Chain Reaction (qPCR)

Total RNA was extracted from the treated cells using TRIzol reagent (catalog number: 15596026, Thermo Fisher Scientific, Waltham, MA, USA) and subsequently converted into cDNA employing PrimeScript™ RT kit (04897030001, Thermo Fisher Scientific, Waltham, MA, USA). Glyceraldehyde-3-phosphate dehydrogenase (*GAPDH*) was used as an internal reference. qPCR was performed using a master mix, and the relative transcription levels were assessed utilizing the $2^{-\Delta\Delta Ct}$ method. However, the corresponding cDNA sequences were downloaded from GeneBank, and the primers were synthesized by Shanghai Sangong Biotechnology Co., Shanghai. The primers used in qPCR are listed in Table 1.

Western Blot

The cells were lysed at 4 °C for 30 minutes, centrifuged at 10,000 rpm/min, and the resulting supernatant was collected. The cell lysate containing total protein was heated and resolved through SDS-PAGE for 3 hours. Subsequently, the proteins were transferred onto membranes and blocked for 1 hour. After this, the membranes were incubated overnight with primary antibodies, including anti-*UBE2H* (ab124593, Abcam, Cambridge, UK, 1:500), anti-*p53* (ab61241, Abcam, Cambridge, UK, 1:500), anti-CASP1 (ab276116, Abcam, Cambridge, UK, 1:500), and anti-GAPDH (sc-17835, Santa Cruz Biotechnology, Shanghai, China, 1:4000). The next day, membranes were washed and underwent incubation with second antibody (ab205719, Abcam, Cambridge, UK, 1:500) at room temperature for 1 hour. The grayscale values of protein bands were determined using Image-Pro Plus (version 6.0, Media Cybernetics, Rockville, MA, USA). Moreover, protein bands were quantified using the Odyssey infrared imaging system (LI-COR Biosciences, Lincoln, NE, USA). GAPDH was employed as an internal control.

Statistical Analysis

Statistical analyses were conducted using SPSS 20.0 (SPSS, Chicago, IL, USA) software. Each experiment was independently repeated three times. The data were presented as the mean ± SEM. The correlation analysis was performed using R software (version 4.0.1, R Foundation for Statistical Computing, Vienna, Austria) with ggplot2 and ggpubr. Furthermore, the differences between multiple groups were assessed using a one-way ANOVA, and post hoc analysis was performed using the Tukey test. A $p < 0.05$ was considered statistically significant.

Results

UBE2H Downregulated in Ischemic Stroke

We established a stroke model to examine the role of *UBE2H* in brain I/R injury and observed a gradually decreasing trend in the *UBE2H* levels during the occurrence and progression of stroke (Fig. 1A,B). Furthermore, the GSE97537 dataset indicated significantly decreased *UBE2H* expression following ischemic stroke (Fig. 1C). Furthermore, to investigate the cell types exhibiting downregulated expression of *UBE2H* following MCAO, microglia and neuronal cells were cultured and subjected to OGD/R. We observed a gradual reduction in the *UBE2H* level in microglia with the prolongation of OGD/R (Fig. 1D,E). These findings suggest that *UBE2H* undergoes downregulation after ischemic stroke.

Overexpression of UBE2H Induced Pyroptosis in Microglia under OGD/R.

We overexpressed *UBE2H* in microglia to explore its role in cell viability. Initially, the overexpression of *UBE2H* in cells demonstrated the successful construction of a mouse model (Fig. 2A,B). CCK-8 assay showed that elevated *UBE2H* levels in the OGD/R model significantly increased the viability of microglia (Fig. 2C). Furthermore, Kyoto Encyclopedia of Genes and Genomes (KEGG) path-

Journal of
BIOLOGICAL REGULATORS
and Homeostatic Agents

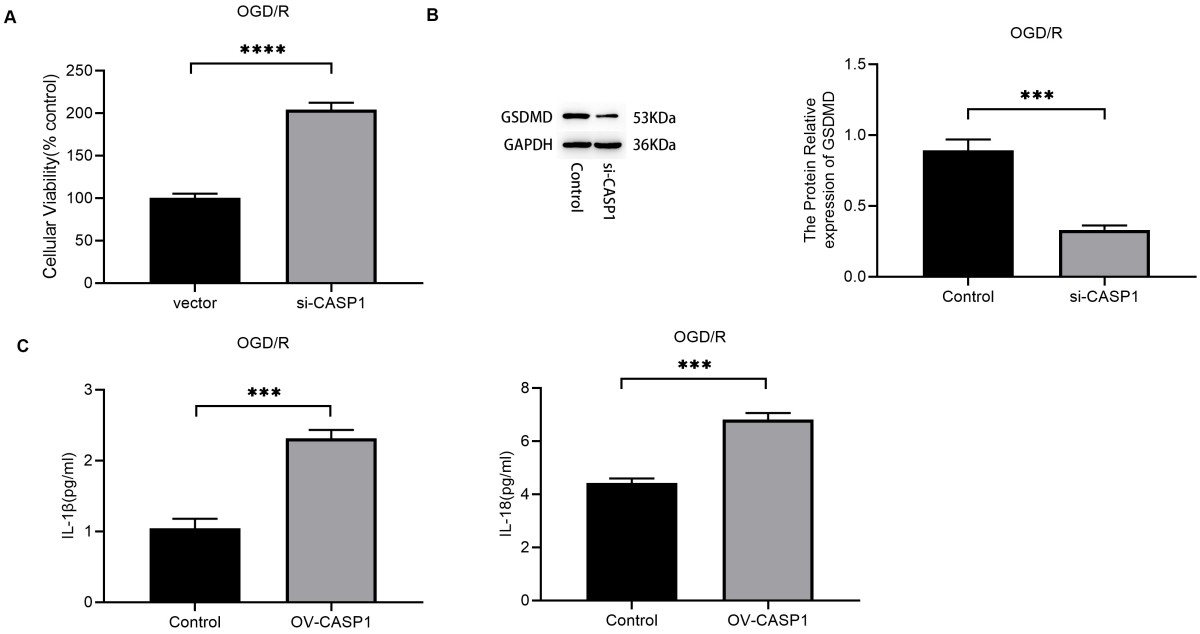

Fig. 4. *CASP1* induced pyroptosis in microglia under OGD/R conditions. (A) Cell viability in each group of cells. (B) Western blot analysis of GSDMD. (C) Evaluation of interleukin-1 beta (IL-1β) and IL-18 levels using Enzyme-Linked Immunosorbent Assay (ELISA). n = 6, ***$p < 0.001$, ****$p < 0.0001$.

way analysis revealed a negative association between pyroptosis and *UBE2H* expression (Fig. 2D). Based on the molecular characteristics of *UBE2H* and the regulation of *p53* by siRNA in turbot, it is speculated that *UBE2H* might be correlated with *p53*. Our findings indicated increased *p53* expression in microglia under OGD/R conditions (Fig. 2E,F). Moreover, we observed that *UBE2H* overexpression significantly downregulated *p53* (Fig. 2G). Additionally, western blot (WB) analysis demonstrated an elevation in *p53* ubiquitination after *UBE2H* overexpression (Fig. 2G).

UBE2H may Regulate Pyroptosis in Microglial through CASP1

Studies have shown that CASP1 may affect cell viability through the pyroptosis pathway. Similarly, we found a correlation between *UBE2H* and CASP1 (cor = –0.883, $p = 0.008$, Fig. 3A). Therefore, we explored whether *UBE2H* regulates cell viability in microglia through pyroptosis. The results indicated that microglia exhibited higher *CASP1* expression under OGD/R conditions (Fig. 3B,C). Subsequently, we assessed the impact of *UBE2H* on the stability of *CASP1* using western blot analysis and observed that overexpression of *UBE2H* significantly reduced the levels of *CASP1* as well as affected the expression of the cytoplasmic division protein Gasdermin D (GSDMD). Additionally, the ubiquitination of *CASP1* was increased in microglia overexpressing *UBE2H* (Fig. 3D).

CASP1 Induced Pyroptosis in Microglia under OGD/R Conditions

We investigated the role of *CASP1* in microglia-mediated pyroptosis response using *CASP1* knockout (si-*CASP1*). The findings demonstrated increased cell viability following *CASP1* knockout (Fig. 4A). However, the levels of GSDMD decreased following *CASP1* knockout (Fig. 4B), indicating that interfering with *CASP1* can reduce pyroptosis in microglia under OGD/R conditions. Furthermore, we investigated the levels of pyroptosis indicators interleukin-1 beta (IL-1β) and interleukin-18 (IL-18) (Fig. 4C) and observed that overexpression of *CSAP1* significantly increased the activity of these indicators in microglia under OGD/R conditions. These findings suggested that *CASP1* can affect the pyroptosis in microglia induced by OGD/R.

UBE2H Induced Pyroptosis in Microglia through CASP1

Under OGD/R conditions, *CASP1* and *UBE2H* were overexpressed in microglia to assess the role of *UBE2H* in the regulation of pyroptosis by inhibiting *CASP1* expression. CCK-8 indicated a significant reduction in the proliferation of cells co-overexpressing *CASP1* and *UBE2H* (Fig. 5A). These findings speculate that *UBE2H* may regulate cell pyroptosis through *CASP1*. After overexpressing *UBE2H* and *CASP1* simultaneously, the release of GSDMD increased (Fig. 5B), along with the secretion of pyroptosis signaling molecules interleukin-1 beta (IL-1β) and IL-18 (Fig. 5C).

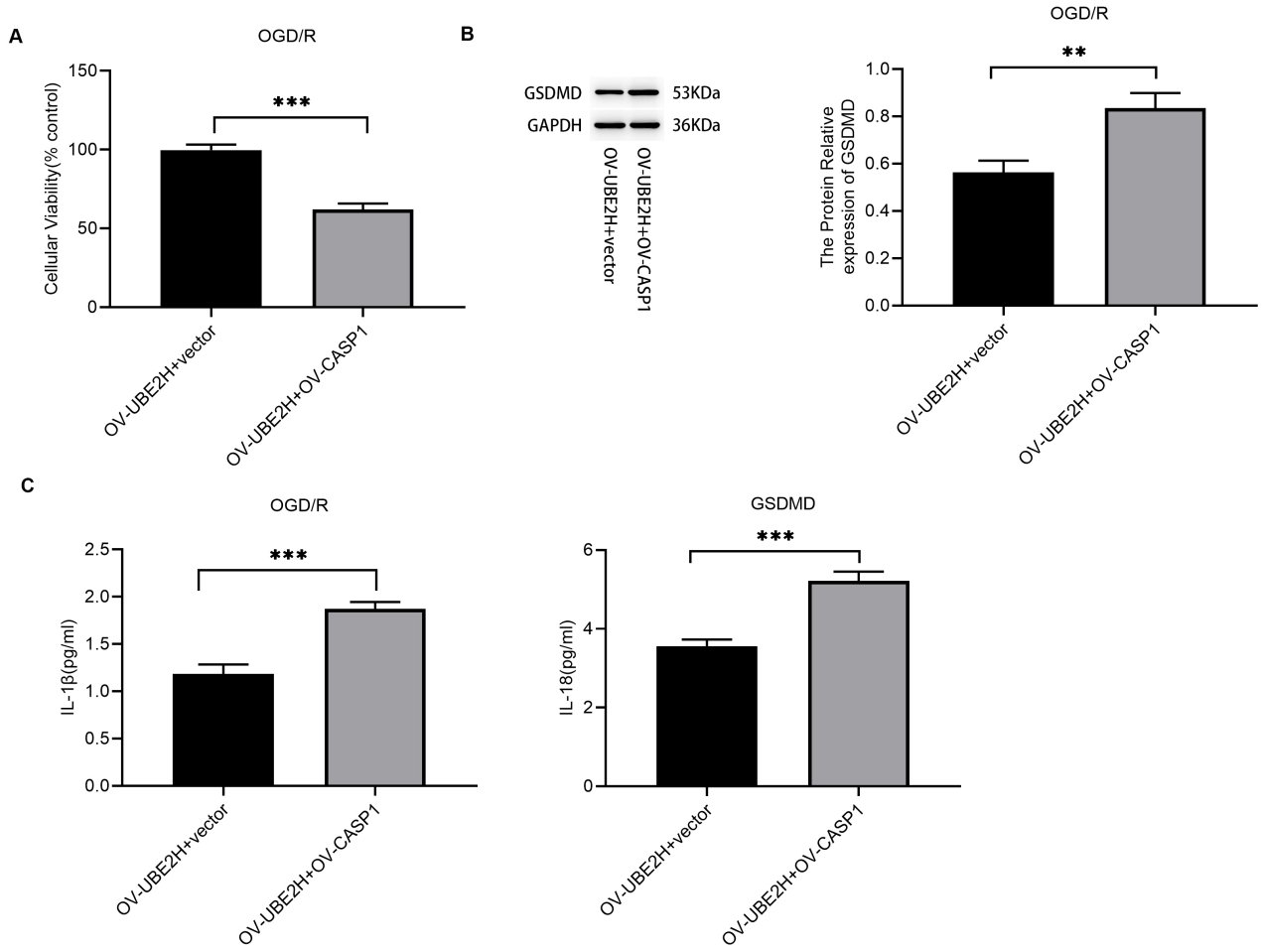

Fig. 5. *UBE2H* induced pyroptosis in microglia through *CASP1* expression. (A) The cell viability levels of each group of cells. (B) Western blot analysis of GSDMD. (C) Evaluation of IL-1β and IL-18 levels using ELISA. n = 6, $^{**}p < 0.01$, $^{***}p < 0.001$.

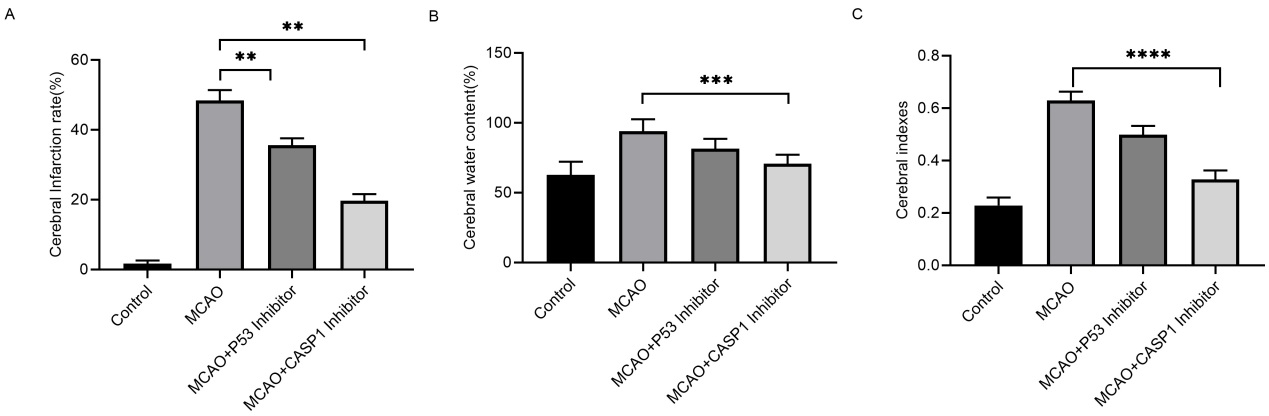

Fig. 6. Inhibitors of *p53* and *CASP1* exhibited a potential therapeutic impact on ischemic stroke. (A) Quantitative map of incidence of cerebral infarction (n = 6). (B) Cerebral water content. (C) Cerebral indexes. n = 6, $^{**}p < 0.01$, $^{***}p < 0.001$, $^{****}p < 0.0001$.

Inhibitors of p53 and CASP1 Exhibited Potential Therapeutic Impact on Ischemic Stroke

We established the experimental stroke model group, blank group, experimental stroke model *p53* inhibitor group, and experimental stroke model+*CASP1* inhibitor group through MCAO surgery. We observed that Inhibitors targeting *p53* and *CASP1* effectively reduced the degree of stroke (Fig. 6).

Journal of
BIOLOGICAL REGULATORS
and Homeostatic Agents

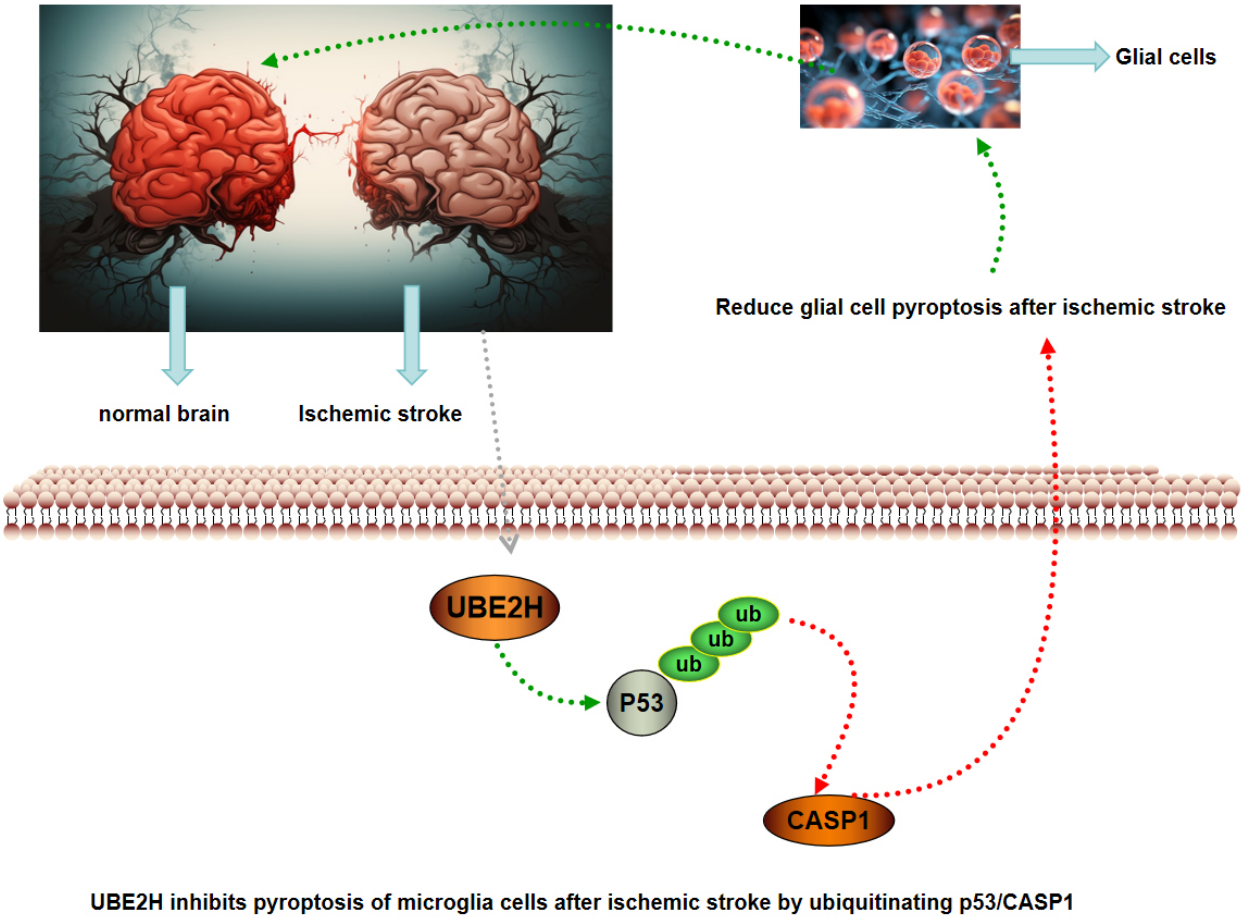

Fig. 7. ***UBE2H*** **inhibits microglial cell pyroptosis following ischemic stroke through ubiquitination of** ***p53/CASP1*** **(Adobe Illustrator software (version CC2019, Adobe Systems Incorporated, San Jose, CA, USA)).**

Discussion

When blood clots or plaques block the arteries supplying blood to the brain, brain cells experience oxygen and nutrient deficiency, resulting in their death or damage. Pyroptosis is an inflammatory type of cell death that can be triggered by various stimuli, such as ischemia, infection, or oxidative stress [20]. Pyroptosis induces the release of pro-inflammatory cytokines, exacerbating neuroinflammation and neuronal damage after stroke.

Inflammation after a stroke can have beneficial and detrimental effects on the brain and the body. On the positive side, inflammation can help clear the debris and promote tissue repair within the brain. On the other hand, inflammation can also increase damage and impair recovery in the brain and other organs. Target autophagy, a cellular process that facilitates the recycling of damaged molecules and cells, offers a potential strategy for modulating post-stroke inflammation. Autophagy can reduce inflammation by removing harmful substances and enhancing cell survival. However, autophagy may also exert negative effects by promoting cell death and impairing immune function [21]. Therefore, it is crucial to determine the optimal level of autophagy that can benefit individuals suffering from ischemic stroke [22]. Another way to modulate inflammation after stroke involves treating underlying autoimmune disorders, infections, or systemic inflammatory diseases that could increase the risk or severity of ischemic stroke [23]. These conditions may trigger or worsen inflammation after stroke by activating immune cells and releasing inflammatory mediators. By controlling these conditions using appropriate drugs or therapies, ischemic stroke patients may have better outcomes and reduced complications [24].

Furthermore, ubiquitination is a protein degradation pathway where ubiquitin-labeled proteins are degraded by the proteasome [25]. Ubiquitination is not disordered but is highly precise and under proper control. It mainly involves three types of enzymes: E1, E2, and E3. E1 activates ubiquitin and transmits it to E2 [26], which carries ubiquitin and pairs with E3. E3 recognizes target proteins and helps transfer ubiquitin to them. This process may occur once or repetitively, forming ubiquitin chains on the protein [27]. Ubiquitination is crucial in regulating the cell cycle, immune system, DNA repair, and signal transduction. Furthermore, it also helps remove damaged or unwanted proteins [28].

UBE2H is associated with various cellular activities, such as cycle regulation, DNA damage, and cell ptosis. Additionally, it interacts with other proteins, such as *p53*, *CASP1*, and *UBE2D3* [29]. *UBE2H* is particularly significant for brain health. As discussed earlier, it can protect microglia from death or inflammation after stroke by facilitating the degradation of *p53* and *CASP1*. This process can reduce brain damage and improve recovery capabilities [30]. Furthermore, *UBE2H* is associated with neurodegenerative diseases. It plays a pivotal role in regulating the accumulation and clearance of amyloid protein β and α-synaptic Nucleoprotein, both toxic proteins that form clumps in the brain and impair its function [31].

In our study, we initially observed the interaction between *UBE2H* and *CASP1*. The *CASP1* gene is a member of the cysteine protease family and plays a significant role in the inflammatory process [32]. However, *CASP1*-mediated polyposis is closely related to tumor development [33–35]. *CASP1* initiates pyroptosis by cleaving GSDMD, and processing cytoplasmic precursors of IL-1b and IL-18 [9,36,37]. This process is crucial for distinguishing pyroptosis from apoptosis and necrosis. Necrosis is a passive and uncontrolled pathway of death that occurs during extreme conditions such as hypoxia and can trigger inflammation and tissue damage [38]. Apoptosis is a regulated mode of cell death that does not cause inflammatory responses. It consists of both endogenous and exogenous pathways, and activation of caspase-3 can induce cell death through these two pathways [39–41]. Therefore, we examined the expression of *GSDMD*, a focal death Signaling molecule, in *UBE2H*-overexpressing and negative control microglia, indicating that overexpression of *UBE2H* may reduce pyroptosis. Furthermore, this process is accompanied by the ubiquitination of *CASP1* (Fig. 7). Fig. 7 was drawn using Adobe Illustrator software (version CC2019, Adobe Systems Incorporated, San Jose, CA, USA). Collectively, this study suggests that *CASP1* may be a target for *UBE2H* in microglia cells.

Conclusions

In summary, these findings indicate that *UBE2H* inhibits microglial apoptosis after ischemic stroke through ubiquitination of *p53*/*CASP1*. This study provides valuable insights into the response of microglia cells to ischemic injury and offers potential protective strategies against further damage. Additionally, it presents novel targets and drugs that can modulate the ubiquitination process, thereby enhancing the prognosis of patients with ischemic stroke.

Availability of Data and Materials

All experimental data included in this study can be obtained by contacting the first author if needed.

Author Contributions

YW, MG designed the research study. BW and QL performed the research. WJ, YT, MG provided help and advice on the experimental data analysis. QW, LL, and XS analyzed the data. All authors contributed to editorial changes in the manuscript. All authors read and approved the final manuscript. All authors have participated sufficiently in the work and agreed to be accountable for all aspects of the work.

Ethics Approval and Consent to Participate

The study was approved by the Ethics Committee of The Third Affiliated Hospital of Qiqihar Medical University (No. AECC-2022-006).

Acknowledgment

Not applicable.

Funding

Funding for this study was provided by Basic Research Fund for Undergraduate Colleges and Universities in Heilongjiang Province (2022-KYYWF-0802).

Conflict of Interest

The authors declare no conflict of interest.

References

[1] Zhu H, Hu S, Li Y, Sun Y, Xiong X, Hu X, *et al*. Interleukins and Ischemic Stroke. Frontiers in Immunology. 2022; 13: 828447.
[2] Noguchi KS, Moncion K, Wiley E, Morgan A, Huynh E, Beauchamp MK, *et al*. Optimal resistance exercise training parameters for stroke recovery: A protocol for a systematic review. PLoS ONE. 2023; 18: e0295680.
[3] Chen W, Zhang Y, Zhai X, Xie L, Guo Y, Chen C, *et al*. Microglial phagocytosis and regulatory mechanisms after stroke. Journal of Cerebral Blood Flow and Metabolism. 2022; 42: 1579–1596.
[4] Zheng K, Lin L, Jiang W, Chen L, Zhang X, Zhang Q, *et al*. Single-cell RNA-seq reveals the transcriptional landscape in ischemic stroke. Journal of Cerebral Blood Flow and Metabolism. 2022; 42: 56–73.
[5] Qiu YM, Zhang CL, Chen AQ, Wang HL, Zhou YF, Li YN, *et al*. Immune Cells in the BBB Disruption After Acute Ischemic Stroke: Targets for Immune Therapy? Frontiers in Immunology. 2021; 12: 678744.
[6] Maida CD, Norrito RL, Daidone M, Tuttolomondo A, Pinto A. Neuroinflammatory Mechanisms in Ischemic Stroke: Focus on Cardioembolic Stroke, Background, and Therapeutic Approaches. International Journal of Molecular Sciences. 2020; 21: 6454.
[7] Wang Q, Tang XN, Yenari MA. The inflammatory response in stroke. Journal of Neuroimmunology. 2007; 184: 53–68.
[8] Candelario-Jalil E, Dijkhuizen RM, Magnus T. Neuroinflammation, Stroke, Blood-Brain Barrier Dysfunction, and Imaging Modalities. Stroke. 2022; 53: 1473–1486.

[9] Thornberry NA, Bull HG, Calaycay JR, Chapman KT, Howard AD, Kostura MJ, *et al*. A novel heterodimeric cysteine protease is required for interleukin-1 beta processing in monocytes. Nature. 1992; 356: 768–774.

[10] Yuan J, Shaham S, Ledoux S, Ellis HM, Horvitz HR. The C. elegans cell death gene ced-3 encodes a protein similar to mammalian interleukin-1 beta-converting enzyme. Cell. 1993; 75: 641–652.

[11] Gamblin TC, Chen F, Zambrano A, Abraha A, Lagalwar S, Guillozet AL, *et al*. Caspase cleavage of tau: linking amyloid and neurofibrillary tangles in Alzheimer's disease. Proceedings of the National Academy of Sciences of the United States of America. 2003; 100: 10032–10037.

[12] Gaudet P, Livstone MS, Lewis SE, Thomas PD. Phylogenetic-based propagation of functional annotations within the Gene Ontology consortium. Briefings in Bioinformatics. 2011; 12: 449–462.

[13] Cerretti DP, Kozlosky CJ, Mosley B, Nelson N, Van Ness K, Greenstreet TA, *et al*. Molecular cloning of the interleukin-1 beta converting enzyme. Science. 1992; 256: 97–100.

[14] Vousden KH, Lane DP. p53 in health and disease. Nature Reviews. Molecular Cell Biology. 2007; 8: 275–283.

[15] Dikic I, Schulman BA. An expanded lexicon for the ubiquitin code. Nature Reviews. Molecular Cell Biology. 2023; 24: 273–287.

[16] Alzrigat M, Párraga AA, Jernberg-Wiklund H. Epigenetics in multiple myeloma: From mechanisms to therapy. Seminars in Cancer Biology. 2018; 51: 101–115.

[17] Lim KH, Joo JY. Predictive Potential of Circulating Ube2h mRNA as an E2 Ubiquitin-Conjugating Enzyme for Diagnosis or Treatment of Alzheimer's Disease. International Journal of Molecular Sciences. 2020; 21: 3398.

[18] Li YP, Lecker SH, Chen Y, Waddell ID, Goldberg AL, Reid MB. TNF-alpha increases ubiquitin-conjugating activity in skeletal muscle by up-regulating UbcH2/E220k. FASEB Journal. 2003; 17: 1048–1057.

[19] Quadri M, Yang X, Cossu G, Olgiati S, Saddi VM, Breedveld GJ, *et al*. An exome study of Parkinson's disease in Sardinia, a Mediterranean genetic isolate. Neurogenetics. 2015; 16: 55–64.

[20] Zhao Y, Zhang J, Zheng Y, Zhang Y, Zhang XJ, Wang H, *et al*. NAD^+ improves cognitive function and reduces neuroinflammation by ameliorating mitochondrial damage and decreasing ROS production in chronic cerebral hypoperfusion models through Sirt1/PGC-1α pathway. Journal of Neuroinflammation. 2021; 18: 207.

[21] Zhou B, Liu J, Kang R, Klionsky DJ, Kroemer G, Tang D. Ferroptosis is a type of autophagy-dependent cell death. Seminars in Cancer Biology. 2020; 66: 89–100.

[22] Ajoolabady A, Wang S, Kroemer G, Penninger JM, Uversky VN, Pratico D, *et al*. Targeting autophagy in ischemic stroke: From molecular mechanisms to clinical therapeutics. Pharmacology & Therapeutics. 2021; 225: 107848.

[23] Tirandi A, Sgura C, Carbone F, Montecucco F, Liberale L. Inflammatory biomarkers of ischemic stroke. Internal and Emergency Medicine. 2023; 18: 723–732.

[24] Li C, Zhao Z, Luo Y, Ning T, Liu P, Chen Q, *et al*. Macrophage-Disguised Manganese Dioxide Nanoparticles for Neuroprotection by Reducing Oxidative Stress and Modulating Inflammatory Microenvironment in Acute Ischemic Stroke. Advanced Science. 2021; 8: e2101526.

[25] Wang MX, Liuyu T, Zhang ZD. Multifaceted Roles of the E3 Ubiquitin Ligase RING Finger Protein 115 in Immunity and Diseases. Frontiers in Immunology. 2022; 13: 936579.

[26] Lan Q, Gao Y, Li Y, Hong X, Xu P. Progress in ubiquitin, ubiquitin chain and protein ubiquitination. Chinese Journal of Biotechnology. 2016; 32: 14–30. (In Chinese)

[27] Craig A, Ewan R, Mesmar J, Gudipati V, Sadanandom A. E3 ubiquitin ligases and plant innate immunity. Journal of Experimental Botany. 2009; 60: 1123–1132.

[28] Cui J, Sinoway LI. Cardiovascular responses to heat stress in chronic heart failure. Current Heart Failure Reports. 2014; 11: 139–145.

[29] Ma A, Cui W, Wang X, Zhang W, Liu Z, Zhang J, *et al*. Osmoregulation by the myo-inositol biosynthesis pathway in turbot Scophthalmus maximus and its regulation by anabolite and c-Myc. Comparative Biochemistry and Physiology. Part A, Molecular & Integrative Physiology. 2020; 242: 110636.

[30] Ndong D, Chen YY, Lin YH, Vaseeharan B, Chen JC. The immune response of tilapia Oreochromis mossambicus and its susceptibility to Streptococcus iniae under stress in low and high temperatures. Fish & Shellfish Immunology. 2007; 22: 686–694.

[31] Cui F, Liu L, Zhao Q, Zhang Z, Li Q, Lin B, *et al*. Arabidopsis ubiquitin conjugase UBC32 is an ERAD component that functions in brassinosteroid-mediated salt stress tolerance. The Plant Cell. 2012; 24: 233–244.

[32] Siegel RM. Caspases at the crossroads of immune-cell life and death. Nature Reviews. Immunology. 2006; 6: 308–317.

[33] Huang T, Zhang P, Li W, Zhao T, Zhang Z, Chen S, *et al*. G9A promotes tumor cell growth and invasion by silencing CASP1 in non-small-cell lung cancer cells. Cell Death & Disease. 2017; 8: e2726.

[34] Li J, Zhang Y, Ruan R, He W, Qian Y. The novel interplay between CD44 standard isoform and the caspase-1/IL1B pathway to induce hepatocellular carcinoma progression. Cell Death & Disease. 2020; 11: 961.

[35] Hong W, Gu Y, Guan R, Xie D, Zhou H, Yu M. Pan-cancer analysis of the CASP gene family in relation to survival, tumor-infiltrating immune cells and therapeutic targets. Genomics. 2020; 112: 4304–4315.

[36] Gaggero A, De Ambrosis A, Mezzanzanica D, Piazza T, Rubartelli A, Figini M, *et al*. A novel isoform of pro-interleukin-18 expressed in ovarian tumors is resistant to caspase-1 and -4 processing. Oncogene. 2004; 23: 7552–7560.

[37] Shi J, Zhao Y, Wang K, Shi X, Wang Y, Huang H, *et al*. Cleavage of GSDMD by inflammatory caspases determines pyroptotic cell death. Nature. 2015; 526: 660–665.

[38] Elmore S. Apoptosis: a review of programmed cell death. Toxicologic Pathology. 2007; 35: 495–516.

[39] D'Arcy MS. Cell death: a review of the major forms of apoptosis, necrosis and autophagy. Cell Biology International. 2019; 43: 582–592.

[40] Cain K, Bratton SB, Cohen GM. The Apaf-1 apoptosome: a large caspase-activating complex. Biochimie. 2002; 84: 203–214.

[41] Kim JH, Lee SY, Oh SY, Han SI, Park HG, Yoo MA, *et al*. Methyl jasmonate induces apoptosis through induction of Bax/Bcl-XS and activation of caspase-3 via ROS production in A549 cells. Oncology Reports. 2004; 12: 1233–1238.